

AD _____

GRANT NUMBER DAMD17-97-1-7272

TITLE: Breast Images with Diffusing Light Waves

PRINCIPAL INVESTIGATOR: Arjun Yodh, Ph.D.

CONTRACTING ORGANIZATION: University of Pennsylvania
Philadelphia, Pennsylvania 19104-3246

REPORT DATE: September 1998

TYPE OF REPORT: Annual

PREPARED FOR: U.S. Army Medical Research and Materiel Command
Fort Detrick, Maryland 21702-5012

DISTRIBUTION STATEMENT: Approved for public release;
distribution unlimited

The views, opinions and/or findings contained in this report are those of the author(s) and should not be construed as an official Department of the Army position, policy or decision unless so designated by other documentation.

DTIC QUALITY INSPECTED 4

19990929 055

REPORT DOCUMENTATION PAGE

Form Approved
OMB No. 0704-0188

Public reporting burden for this collection of information is estimated to average 1 hour per response, including the time for reviewing instructions, searching existing data sources, gathering and maintaining the data needed, and completing and reviewing the collection of information. Send comments regarding this burden estimate or any other aspect of this collection of information, including suggestions for reducing this burden, to Washington Headquarters Services, Directorate for Information Operations and Reports, 1215 Jefferson Davis Highway, Suite 1204, Arlington, VA 22202-4302, and to the Office of Management and Budget, Paperwork Reduction Project (0704-0188), Washington, DC 20503.

1. AGENCY USE ONLY (Leave blank)	2. REPORT DATE September 1998	3. REPORT TYPE AND DATES COVERED Annual (1 Sep 97 - 31 Aug 98)	
4. TITLE AND SUBTITLE Breast Images with Diffusing Light Waves		5. FUNDING NUMBERS DAMD17-97-1-7272	
6. AUTHOR(S) Yodh, Arjun, Ph.D.			
7. PERFORMING ORGANIZATION NAME(S) AND ADDRESS(ES) University of Pennsylvania Philadelphia, Pennsylvania 19104-3246		8. PERFORMING ORGANIZATION REPORT NUMBER	
9. SPONSORING / MONITORING AGENCY NAME(S) AND ADDRESS(ES) U.S. Army Medical Research and Materiel Command Fort Detrick, Maryland 21702-5012		10. SPONSORING / MONITORING AGENCY REPORT NUMBER	
11. SUPPLEMENTARY NOTES			
12a. DISTRIBUTION / AVAILABILITY STATEMENT Approved for public release; distribution unlimited		12b. DISTRIBUTION CODE	
13. ABSTRACT (Maximum 200 words) <div style="border: 1px solid black; padding: 10px; width: fit-content; margin: 20px auto;">(See page 3)</div>			
14. SUBJECT TERMS Breast Cancer		15. NUMBER OF PAGES 17	
(See page 3)		16. PRICE CODE	
17. SECURITY CLASSIFICATION OF REPORT Unclassified	18. SECURITY CLASSIFICATION OF THIS PAGE Unclassified	19. SECURITY CLASSIFICATION OF ABSTRACT Unclassified	20. LIMITATION OF ABSTRACT Unlimited

FOREWORD

Opinions, interpretations, conclusions and recommendations are those of the author and are not necessarily endorsed by the U.S. Army.

✓ Where copyrighted material is quoted, permission has been obtained to use such material.

✓ Where material from documents designated for limited distribution is quoted, permission has been obtained to use the material.

✓ Citations of commercial organizations and trade names in this report do not constitute an official Department of Army endorsement or approval of the products or services of these organizations.

___ In conducting research using animals, the investigator(s) adhered to the "Guide for the Care and Use of Laboratory Animals," prepared by the Committee on Care and Use of Laboratory Animals of the Institute of Laboratory Resources, National Research Council (NIH Publication No. 86-23, Revised 1985).

___ For the protection of human subjects, the investigator(s) adhered to policies of applicable Federal Law 45 CFR 46.

___ In conducting research utilizing recombinant DNA technology, the investigator(s) adhered to current guidelines promulgated by the National Institutes of Health.

___ In the conduct of research utilizing recombinant DNA, the investigator(s) adhered to the NIH Guidelines for Research Involving Recombinant DNA Molecules.

___ In the conduct of research involving hazardous organisms, the investigator(s) adhered to the CDC-NIH Guide for Biosafety in Microbiological and Biomedical Laboratories.

PI - Signature

Date

13. ABSTRACT:

The goal of our proposed work was to improve the breast tumor diagnostic capabilities of optical spectroscopy and imaging based on diffusing near infrared light. We introduced new theoretical methodologies for image reconstruction within the human breast, and planned to develop these theoretical approaches further, and test these approaches experimentally. The primary benefit derivable from these ideas is improved breast image fidelity, which in turn, would enable clinicians to fully exploit the new spectroscopic and scattering contrast mechanisms available with the optical method for increased tumor sensitivity and specificity. Since submission of this proposal we have experimentally demonstrated the theoretical ideas underlying the near-field Fast Fourier Transform approach. These experiments produced two-dimensional projection images of thin objects embedded in infinite media. The apparatus however, was not well suited for realistic parallel plate soft breast compression geometries, so during the last year we have completed the construction of an instrument that is far better suited for these more realistic studies. We have also explored various theoretical issues including the effects of imaging filters on the reconstructions, and the potential for three-dimensional reconstruction.

14. Subject Terms: Photon-Migration, Photon-Density-Waves, Near-Infrared-Spectroscopy, Fast-Fourier-Transform, Image-Reconstruction, Breast Cancer

TABLE OF CONTENTS

Report Documentation Page	1
FOREWORD	2
ABSTRACT AND SUBJECT TERMS	3
TABLE OF CONTENTS	4
MAIN SECTION	5
Introduction	
Main Body	
Conclusions	
REFERENCES	12
APPENDIX	14

INTRODUCTION

The application of the optical method to breast tumor imaging and specification is attractive for several reasons. The techniques utilize non-ionizing radiation, are non-invasive, and are often technologically simple and fast. These features have lead, in some cases, to compact, portable, and inexpensive clinical instruments in other fields of medicine. In addition the optical method has a great range of measurable parameters that could enhance tumor sensitivity and specificity. For example, the higher metabolic activity of the rapidly growing tumor increases organelle population, particularly mitochondria, which leads to an increasing scattering factor for the tumor. Blood dynamics such as oxygen saturation are expected to be substantially different in the rapidly growing tumor, and will alter optical absorption factors; the optical absorption, fluorescence, and scattering of contrast agents such as indocyanine green that occupy vascular and extravascular space, may also provide useful forms of sensitization.

Optical characterization of the breast has been attempted since 1929 [Cutler, 1929] when the term "diaphanography" was applied to shadow graphs of breast tissue. Although the method has been tested over the years on some 2000 patients, the method was largely inadequate for clinical use since it was difficult to separate the effects of absorption and scattering within the tissue. Typical photon random walk steplengths in tissues are in the range of 1 mm (corresponding to a reduced scattering coefficient of 10 cm^{-1}) for photons in the near infrared (i.e. $\sim 800\text{ nm}$). Even in the region of low tissue absorption (i.e. between 600 nm and 1300 nm), this high degree of scattering tends to distort spectroscopic information and blur optical images as a result of the large distribution of photon pathways through the tissue that contribute to measured signals.

A recent and critical advance in the photon migration field however, [see papers and references in Chance & Alfano, 1995; Yodh & Chance, 1995], has been the recognition and widespread acceptance that light transport over long distances in tissues is well approximated as a diffusive process. Using this basic physical model, it is possible to quantitatively separate tissue scattering effects from tissue absorption effects, and one can accurately incorporate the effects of boundaries, such as the air-tissue interface, into the transport theory [Patterson et al., 1991a, 1991b]. Waves of diffuse light energy density [Gratton, 1990] (or their time-domain analogs [Patterson et al., 1989; Delpy et al, 1988; Jacques, 1989; Benaron & Stevenson, 1993]) are generated, and propagate deeply in tissues (i.e. as much as 10 cm) while obeying simple optical rules such as refraction [O'Leary et al., 1992], diffraction [Boas et al., 1993; Fishkin & Gratton, 1993], interference [Schmitt et al., 1992], and dispersion [Tromberg et al., 1993; Sevick et al., 1992] as they encounter variations in tissue optical properties.

The promise of the optical method has led to the first clinical studies of the optical technique in the human breast. In these experiments [Franceschini et al., 1996; Fantini et al., 1996] diffusive waves were applied to the human breast in the transmission mode in a conventional X-ray "hard compression" parallel plate source-detection geometry. The team obtained wave amplitude and phase-shift data, and then processed the data using a phase-corrected linear backprojection approach [Fantini et al., 1996]. The inversion procedure did not separate scattering from absorption, and furthermore, the inversion model was extremely approximate. Nevertheless the method gave images of ~ 1 cm diameter tumors in roughly 60-70 % of the cases [Fantini et al., 1996] which were congruent with X-ray mammography of the same breast. There were also important exceptions, but the results are the first, and clearly indicate the technique is potentially very important and that further investigation is required.

In order to fully realize the potentialities of the optical method for breast cancer imaging it is crucial to separate spectroscopic and scattering variations with high fidelity. Imperfect quantitation will severely limit both the sensitivity and specificity of the technique. Complete information about breast tumor shapes and optical properties require tomographic approaches to the data acquisition and inversion. There has been extensive image reconstruction work with diffusive waves along these lines during the last few years [see for example van Houten et al., 1996; Ishii et al., 1995; Chang et al., 1995; Arridge et al., 1991; Pogue et al., 1995; O'Leary et al., 1995]. In essentially all of these approaches a perturbative model (either Born or Rytov approximation) is employed to define the forward problem. Then the sample volume is discretized, voxel weights are assigned, and variations in absorption and scattering factors within the sample are obtained by some iteration or single-value decomposition procedure. In our lab, for example, we have experimentally demonstrated the tomographic reconstruction of absorptive and scattering heterogeneities in tissue phantoms [O'Leary et al., 1995; O'Leary SPIE], we have shown how to reconstruct lifetime and concentration of fluorophores in tissues [O'Leary et al., 1996a], we have reconstructed the dynamical flow properties within turbid media using diffused temporal light field correlation functions [Boas et al., 1995], and we have demonstrated a technique whereby structural information from a second imaging modality (such as X-Ray, ultrasound, or MRI) may be optimally combined with the photon migration techniques to yield more accurate optical properties [O'Leary et al., 1996b].

In this research program, we proposed to develop and test new theoretical algorithms for breast imaging instruments based on the use of diffuse photon density waves. One scheme, the near-field Fast Fourier Transform (FFT) approach, affords a rapid method for imaging of tissue interiors, and thus will be useful for on-line analysis of the breast images. The second scheme, the non-perturbative approach, is a novel method for the inclusion of boundary effects, and the computation of absorption and scattering factors to high order;

importantly this scheme does not involve matrix inversion and, as a result of its repeated integrations, is expected to be less susceptible to experimental noise. If successful these powerful theoretical methods are expected to improve the fidelity of the breast images, and it is anticipated that the anatomical information generated by the device will be useful for improving our ability to specify the nature of breast tumors.

BODY

We have implemented several aspects of the proposed work during the past year. Most of this work has been connected with the near-field FFT theoretical approach, although all of the instrument development will be useful to both theoretical approaches. We briefly review these developments here.

Experimental Demonstration of Main Theoretical Ideas Underlying the Near-field Fast Fourier Transform Approach [Li97, Li98]:

In order to demonstrate the feasibility of this algorithm, we have performed amplitude and phase measurements in a plane parallel geometry shown schematically in Figure 1 below.

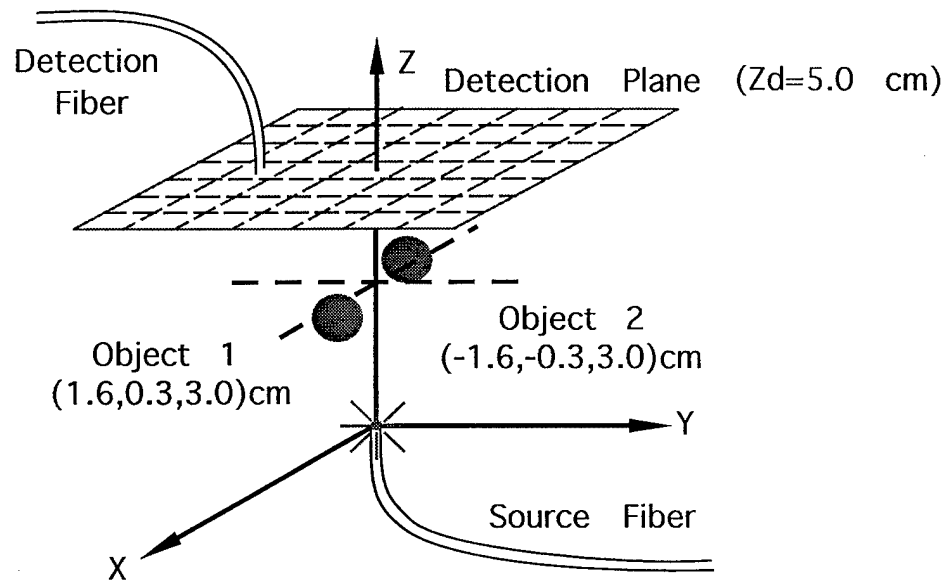


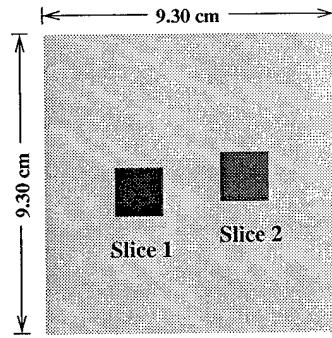
Figure 1 : Illustration of the experimental geometry: the source is fixed at the origin and the detector scans in a planar geometry at $z=z_d=5.0$ cm over a 9.3×9.3 cm² region in x-y step sizes of 0.3 cm. The optical heterogeneities are embedded in the highly scattering medium between the source and the detection plane.

The entire experiment was embedded in an effectively infinite sample of Intralipid so that infinite media boundary conditions could be safely employed. In order to carry out these experiments we developed a rapid homodyne detection systems based upon In-phase/In-quadrature demodulation techniques. Much of the experimental and theoretical details are described in our publication [Li97] which is included as an Appendix to this report.

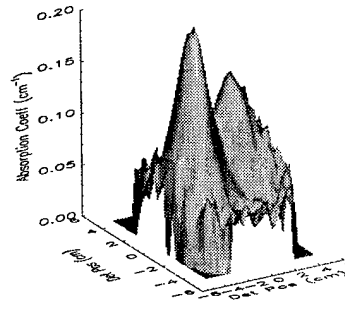
The demonstration was carried out using $\sim 3\text{mW}$ of light at 786 nm . Light from the diode laser was amplitude modulated at 100 Mhz and fiber coupled into the fishtank containing the Intralipid (with scattering factor of about 7.3 cm^{-1}). Scanning of the detector fiber was made in steps of about 0.3 cm . The amplitude and phase of the transmitted diffuse photon density waves were thus recorded at 1024 points on the detection plane. In these test experiments we first measured the signals with a uniform background, and then we placed two heterogeneities (absorbing or scattering) into the medium, remade the measurements, and extracted the projection images of medium optical properties with the FFT technique.

Theoretically, the technique consists of several steps. After measuring the "total" diffuse photon density waves (due to the heterogeneities plus background), we subtracted off the "background" wave to obtain the "scattered wave". The scattered wave is then spatially fourier transformed in the plane of detection. The FFT method formally relates the fourier transform of the scattered wave to a weighted sum of the fourier transforms of the so-called tumor function; the tumor function essentially contains all of the information about the sample heterogeneities such as their position, size and optical properties. For relatively thin heterogeneities we select a plane (or slice), parallel to the detection plane but within the sample volume, that best approximates the position of the heterogeneities. Then a simple algebraic operation and an inverse-FFT generates an two-dimensional projection image.

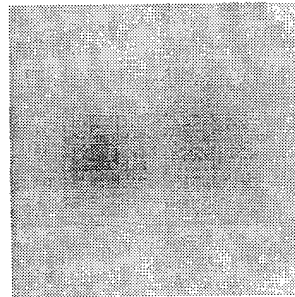
We demonstrated this method in [Li97], and the results for two absorbing heterogeneities are shown in Figure 2. The method was shown to work for absorbing and scattering objects [Li97]. However for extended objects (i.e. with diameters larger than a few random walk steps) we found that the absolute optical properties were incorrect, though the relative optical properties were still quite accurate. This is due to the breakdown of the thin slice approximation, and requires three-dimensional reconstruction techniques.



(a)



(b)



(c)

Figure 2 : (a) shown the exact x-y positions of the two thin absorbing slices. (b) shows the reconstructed 2-D photographic image of these two slices using the K-space spectrum analysis algorithm. (c) shows the surface plots of the reconstructed images where the reconstructed absorption variations ($\delta\mu_a^{rec}$) can be found.

New Instrumentation for More Realistic Compressed Breast Geometries:

There are many improvements that must be made upon the work described above [Li97] before the FFT methods can be moved to the clinic. First and foremost, we need an instrument designed to work in a realistic geometry. Secondly we need more rapid and flexible scanning at multiple optical wavelengths.

Over the past six months we have developed such a device. We designed the instrument onto a bed-like frame built of light-weight aluminum strutting. The table is lockable and also has removable wheels. The rigid frame is critical to eliminate positioning errors. We have built into the frame a two-plate, soft-compression optical mammogram unit. One of the plates has a source grid of 12 fibers embedded into the compression plate. By comparison to our single source systems, we have more flexibility to define our scan region, and we anticipate that we will need multiple source positions for the true three-dimensional reconstructions. The other critical problem we have addressed in the current instrument is offset drift. In particular for every measurement we optically multiplex between a 750 nm, an 786 nm, and a "dark" measurement. This allows us to continually subtract off electronic DC offsets.

On the detection side we still use stepper motors to scan a 9cm x 9cm detection plate in 0.6 cm increments (flexible). The previous scanning system was fragile at best. The current one is much more robust. In addition we have added in an electronically controllable attenuator into the signal path before the demodulator in order to increase the linear dynamic range of the device.

In addition to building the new instrument we have carried out a series of meticulous tests in order to correct for systematic amplitude and phase shifts in the electronics and to discover our limitations due to positional noise. These phantom tests are underway in parallel with theoretical improvements.

Theoretical Studies:

We have implemented several improvements in our theoretical approach. The first problem we have addressed concerns the true slab geometry. In particular we have determined and incorporated the slab geometry Green's Functions into the original FFT theory. This has lead, for example, to considerably better agreement with analytical theory. The detailed theoretical formulas are extensive, but may be found in Xingdi Li's thesis [Li98].

Another problem that is often glossed over in the literature, but that we have found to be very important is the use of processing "filters." We have initiated a systematic investigation of the effects of various filters. Generally we find that the use of some sort of filtering is crucial to reduce reconstruction artifacts. Examples of filters used are: low pass filters on the detection (k -space) grid data, Hamming filters on the tumor function (perturbation), and

Hamming filters on the reconstructed images in real space. Unfortunately each of these filters also introduces artifacts. For example, the reconstructed optical properties are generally reduced by 50%. Our hope is to understand these artifacts, correct for them, and thus optimally use the processing filters.

The last critical theoretical issue concerns full three-dimensional reconstruction with the methods. This requires the greatest amount of new insight. We have formally developed (unpublished) an approach which uses multiple input plane waves to generate 3-D images. Of course plane wave sources are not very realistic. On the other hand we believe the our new 12 source compression plate offers the possibility for a related 3-D approach, because each point source can be considered to be built from many plane waves. Much theoretical work remains on this for the next year.

CONCLUSIONS

We have accomplished a lot since submission of this proposal. First we demonstrated by experiment [Li97] the validity of the FFT image reconstruction approach. These experiments were carried out under ideal (i.e. infinite media, etc.) conditions however. To this end we have put together that works in more realistic scenerios such as the compressed breast geometry. This apparatus will be useful for realistic phantom studies, and eventually (not in this granting period) for optical mammography in the clinic. The new apparatus has solved many of the early technical problems we had with the old instrument including the problem of IQ-chip offset drift, multiple wavelengths for spectroscopy (we now have multiple wavelengths), and many mechanical instabilities are now corrected. On the theoretical side we have implemented slab Green's Functions into the FFT treatment, and are systematically exploring the use of processing filters. We are just beginning to tackle the full 3-D FFT theory; this will be our most difficult task for the next funding period. No work was done on the Auxilliary function approach, becuase the other project was going so well. We hope to consider this theory also in the next year.

REFERENCES

- Arridge, S., P. van der Zee, M. Cope, and D. Delpy, in *Time Resolved Spectroscopy and Imaging in Tissues* (SPIE Optical Engineering Press, Bellingham, WA, 1991) Vol. 1431, p.204.
- Benaron, D.A., and Stevenson, D.K., Optical time of flight and absorbance imaging of biologic media, *Science* **259**, 1463-1466 (1993).
- Boas, D.A., O'Leary, M.A., Chance, B. and Yodh, A.G., Scattering and wavelength transduction of diffuse photon density waves, *Phys. Rev. E* **47**, R2999-3003 (1993).
- Boas, D.A., L.J. Campbell, and A.G. Yodh, Scattering and Imaging with Diffusing Temporal Correlations, *Phys. Rev. Lett.* **75**, 1855-59 (1995).
- Chance, B., and Alfano, R.R., *Proceedings of Optical Tomography, Photon Migration, and Spectroscopy of Tissue and Model Media: Theory, Human Studies, and Instrumentation* Vol. I,II, SPIE **2389** (1995).
- Chang, J., Graber, H., and Barbour, R.L., in *Image Reconstruction of Dense Scattering Media Using Constrained CGD and a Matrix Scaling Technique* (SPIE Optical Engineering Press, Bellingham, WA 1995), pp. 682-91.
- Cutler, M., *Surgery, Gynecology and Obstetrics* **48**, 721 (1929).
- Delpy, D.T., Cope, M., Zee, P. van de, Arridge, S., Wray, S., and Wyatt, J., Estimation of optical pathlength through tissue from direct time of flight measurement, *Phys. Med. Biol.* **33**, 1433-1442 (1988);
- Fantini, S., Franceschini, M.A., Gaida, G., Gratton, E., Jess, H., Mantulin, W.M., Moesta, K.T., Schlag, P.M., and Kashke, M., Frequency-domain optical mammography: Edge effect corrections, *Med. Phys.* **23**, 1-9 (1996).
- Fishkin, J. and Gratton, E., Propagation of photon density waves in strongly scattering media containing an absorbing "semi-infinite" plane bounded by a straight edge, *J. Opt. Soc. Am. A* **10**, 127-140 (1993).
- Franceschini, M.A., Moesta, K.T., Fantini, S., Gaida, G., Gratton, E., Jess, H., Seeber, M., Schlag, P.M., Kashke, M., Frequency-domain techniques enhance optical mammography: initial clinical results, *Proc. of Nat. Ac. of Sci.* (submitted 1996).
- Gratton, E., Mantulin, W., Ven, M. J. van de, Fishkin, J., Maris, M. and Chance, B., in *Proceedings of The Third International Conference: Peace through Mind/Brain Science*, August 5-10, 1990, Hamamatsu, Japan, 183-189 (1990).
- Ishii, M., J. Leigh, and Schotland, J., in *Optical Tomography, Photon Migration and Spectroscopy of Tissue and Model Media: Theory, Human Studies and Instrumentation* (SPIE Optical Engineering Press, Bellingham, WA 1995), pp. 312.
- Ishimaru, A. *Wave Propagation and Scattering in Random Media* (Academic, New York, 1978).
- Jacques, S.L., Time resolved propagation of ultrashort laser pulses within turbid tissues, *Appl. Opt.* **28**, 2223-2229 (1989).
- Li97, X.D. Li, T. Durduran, A.G. Yodh, B. Chance, and D. Pattanayak, Diffraction Tomography for Biomedical Imaging with Diffuse Photon Density Waves, *Opt. Lett.* **22**, 573 (1997).
- Li98 PhD Thesis, University of Pennsylvania (1998).
- O'Leary, M.A., Boas, D.A., Chance, B. and Yodh, A.G., Refraction of diffuse photon density waves, *Phys. Rev. Lett.* **69**, 2658-2661 (1992).
- O'Leary, M.A., Boas, D.A., Chance, B. and Yodh, A.G., Experimental images of heterogeneous turbid media by frequency-domain diffusing-photon tomography, *Optics Letters* **20**, 426-428 (1995).
- O'Leary, M.A., Boas, D.A., Chance, B., and Yodh, A.G., Images of Inhomogeneous Media Using Diffuse Photon Density Waves, *Opt. Soc. Am. Proceedings on Advances in Optical Imaging and Photon Migration* **21**, 106 (1994).
- O'Leary, M.A., Boas, D.A., Li, X.D., Chance, B. and Yodh, A.G., Fluorescence Lifetime Imaging in Turbid Media, *Optics Letters* **21**, 158-60 (1996a).
- O'Leary, M.A., Ntzitachristos, V., Chance, B. and Yodh, A.G., Co-registration of Images from Diffusive Waves with other Imaging Modalities to Enhance Optical Specificity, in *Proceedings of Advances in Optical Imaging and Photon Migration*, Orlando, Florida, March (1996b).

- Patterson, M.S., Chance, B. and Wilson, B.C., Time resolved reflectance and transmittance for the non-invasive measurement of tissue optical properties, *Appl. Opt.* **28**, 2331-2336 (1989);
- Patterson, M.S., Chance, B., and Wilson, B.C., Time-resolved reflectance and transmittance for the noninvasive measurement of tissue optical properties. *Appl. Opt.* **28**, 2231-2236 (1991a).
- Patterson, M.S., Moulton, J.D., Wilson, B.C., Berndt, K.W., and Lakowicz, J.R., Frequency domain reflectance for the determination of the scattering and absorption properties of tissue, *Appl. Opt.* **32**, 607-616 (1991b).
- Pogue, B.W., Patterson, M.S., and Farrell, T.J. in *Optical Tomography, Photon Migration and Spectroscopy of Tissue and Model Media: Theory, Human Studies and Instrumentation* (SPIE Optical Engineering Press, Bellingham, WA 1995), pp. 328.
- Schmitt, J.M., Knüttel, A. and Knudsen, J.R., Interference of diffusive light waves, *J. Opt. Soc. Am. A* **9**, 1832 (1992).
- Sevick, E.M., Lakowicz, J., Szmajski, H., Nowaczyk, K. and Johnson, M.L., Frequency domain imaging of absorbers obscured by scattering, *J. Photochem. Photobiol. B* **16**, 169- 185 (1992).
- Tromberg, B., Svaasand, L.O., Tsay, T., and Haskell, R.C., Properties of photon density waves in multiply scattering media, *Appl. Optics* **32**, 607-616 (1993).
- van Houten, J., Benaron, D., Spilman, S., and Stevenson, D., Imaging Brain Injury Using Time-resolved near- infrared light scanning, *Pediatric Research* **39**, 470 (1996).
- Yodanis, C.L., and Chance, B., Spectroscopy and Imaging with Diffusing Light, *Physics Today* **48**, 34-40 (1995).

Diffraction tomography for biochemical imaging with diffuse-photon density waves

X. D. Li, T. Durduran, and A. G. Yodh

Department of Physics and Astronomy, University of Pennsylvania, Philadelphia, Pennsylvania 19104

B. Chance

Department of Biochemistry and Biophysics, University of Pennsylvania, Philadelphia, Pennsylvania 19104

D. N. Pattanayak

GE Corporate Research and Development, Schenectady, New York 12301

Received November 5, 1996

The spatial structure of optically heterogeneous turbid media is probed with diffusive light. Projection images are obtained experimentally by deconvolution of the scattered diffuse-photon density waves on a planar boundary by use of a fast Fourier transform. The method is very fast, permitting object localization and characterization in ~ 1000 volume-element samples on subsecond computational time scales. The optical properties of slice-shape inhomogeneities are accurately determined. © 1997 Optical Society of America

Recently the application of near-IR diffusing light for biomedical diagnosis and imaging has gained favor because of its noninvasive nature, economy, and novel contrast relative to other diagnostics.¹⁻³ To this end a variety of techniques for imaging with diffuse light have been explored.^{4,5} Most methods use direct matrix inversion (e.g., singular-value decomposition) or iterative techniques (e.g., algebraic reconstruction-simultaneous iterative reconstruction technique,⁶ conjugate gradient descent) for image reconstruction.

Here we introduce a new near-field, diffusive-wave-imaging methodology, using techniques similar to those of conventional diffraction tomography.⁷ The near-field diffraction tomography method has attracted the attention of a few researchers in the photon-migration field.⁸ In this Letter present a rigorous account of the theory and provide the first experimental images of absorbing and scattering objects in turbid media obtained by this approach. The method differs from least-squares techniques⁶ in that it is fast and noniterative. In addition to providing information about the position and shape of a hidden object or objects, *projection* images can be used to deduce the optical properties of heterogeneities without the need for complex reconstruction procedures such as matrix inversion when the heterogeneities are thin and information on their depth is available.

We adopt the frequency-domain picture for our discussion. An intensity sinusoidally modulated light source coupled into a highly scattering medium such as tissue produces a diffuse-photon density wave (DDPW) that propagates outward from the source.⁹ The amplitude and phase of this DPDW depend on the absorption and the scattering coefficients within the turbid medium.

In uniform turbid media the DPDW from a point source at \mathbf{r}_s detected at position \mathbf{r}_d has the form $U_0(\mathbf{r}_d, \mathbf{r}_s, \omega) = M_0 \exp(ik_0|\mathbf{r} - \mathbf{r}_s|)/(4\pi D_0|\mathbf{r} - \mathbf{r}_s|)$. Here ω is the angular source-modulation frequency, M_0 is the ac amplitude of the source, $D_0 = v/(3\mu_{so}')$

is the diffusion coefficient (v is the speed of light in the medium), $k_0 = [(-\mu_{a0}v + i\omega)/D_0]^{1/2}$ is the DPDW wave number, and μ_{a0} and μ_{so}' are, respectively, the homogeneous absorption and the reduced scattering coefficients of the medium. In heterogeneous media, the total DPDW, $U_t(\mathbf{r}_d, \mathbf{r}_s, \omega)$, is a superposition of incident $[U_0(\mathbf{r}_d, \mathbf{r}_s, \omega)]$ and scattered $[U_1(\mathbf{r}_d, \mathbf{r}_s, \omega)]$ DPDWs. To the first order in the variation of optical absorption and reduced scattering coefficients, the scattered wave is

$$U_1(\mathbf{r}_d, \mathbf{r}_s, \omega) = \int_V T[U_0(\mathbf{r}, \mathbf{r}_s, \omega)]G(|\mathbf{r}_d - \mathbf{r}|)d^3r. \quad (1)$$

Here $G(|\mathbf{r}_d - \mathbf{r}|)$ is the Green's function for the DPDW in the homogeneous medium. We call $T[\mathbf{r}, U_0(\mathbf{r}, \mathbf{r}_s, \omega)]$ the inhomogeneity function. $T_{\text{abs}}[\mathbf{r}, U_0(\mathbf{r}, \mathbf{r}_s, \omega)] = (\delta\mu_a(\mathbf{r})v/D_0)U_0(\mathbf{r}, \mathbf{r}_s, \omega)$ for absorbing objects, and $T_{\text{scatt}}[\mathbf{r}, U_0(\mathbf{r}, \mathbf{r}_s, \omega)] = [\delta\mu_s'(\mathbf{r})3D_0k_0^2/v - \nabla \ln(\delta\mu_s' + \mu_{so}')] \cdot \nabla U_0(\mathbf{r}, \mathbf{r}_s, \omega)$ for scattering objects. The integral is over the sample volume V .

We consider a parallel-plane geometry [Fig. 1(a)] that is potentially applicable to the compressed-breast configuration. For this case, a natural basis set for the Green's function in Eq. (1) is the simple Weyl expansion form in terms of spatial frequencies p, q, m ¹⁰:

$$G(|\mathbf{r}_d - \mathbf{r}|) = \frac{i}{8\pi^2} \int_{-\infty}^{\infty} \int_{-\infty}^{\infty} \frac{dpdq}{m} \exp[ip(x_d - x) + iq(y_d - y) + im(z_d - z)], \quad (2)$$

where we assume that $z_d > z$ without losing generality; $m = (k_0^2 - p^2 - q^2)^{1/2}$ with $\text{Im}(m) > 0$. Using Eq. (2) and taking the two-dimensional (2D) spatial Fourier transform of both sides of Eq. (1) [with respect to transverse (x, y) coordinates], we obtain

$$\tilde{U}_1(p, q, z_d, \mathbf{r}_s, \omega) = \frac{i}{2m} \int_{z_s}^{z_d} \tilde{T}(p, q, z, \mathbf{r}_s, \omega) \times \exp[im(z_d - z)]dz. \quad (3)$$

The left side of Eq. (3) is the 2D Fourier transform of

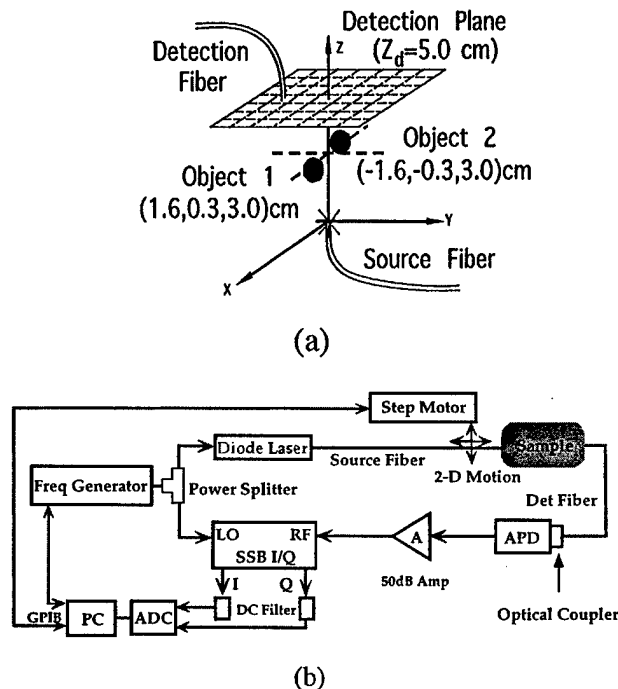


Fig. 1. (a) Experimental geometry: The source is fixed at the origin, and the detector scans in a planar geometry at $z = z_d = 5.0$ cm over a 9.3 cm \times 9.3 cm region. (b) Setup: APD, avalanche photodiode; A, amplifier; SSB I/Q, single-sideband in-phase/quadrature-phase demodulator; LO, local port; RF, radiofrequency port; ADC, analog-digital converter; GPIB, general purpose interface bus.

the scattered DPDW measured on the detection plane $z = z_d$. This integral equation is approximated by

$$\sum_{j=1}^N \tilde{T}(p, q, z_j, \mathbf{r}_s, \omega) \exp(-imz_j) = \frac{2m}{i\delta z} \exp(-imz_d) \tilde{U}_1(p, q, z_d, \mathbf{r}_s, \omega), \quad (4)$$

where δz is the discretized step size and N is the total number of slices in the z direction.

For the projection image, we replace z_j on the left side of Eq. (4) with the estimated slice position of the object. We drop the sum over all other z_j 's and then perform a 2D inverse Fourier transform of \tilde{T} to obtain the projection image. When the object thickness is of the order of several transport mean free paths [$1/(\mu_a + \mu_s')$], we can deduce accurately the optical properties of the object or objects. For thicker objects (i.e., >5 mm), the average over the size of the object weighted by the sum of exponential phase factors reduces the accuracy of the optical properties. However, position information is accurate, and the relative optical properties of multiple objects are also very accurate.

To demonstrate the feasibility of this algorithm, we performed amplitude and phase measurements in a parallel-plane geometry [Fig. 1(a)]. The experimental setup is shown in Fig. 1(b). The system consists of a rf-modulated (100-MHz), low-power (~ 3 -mW) diode laser operating at 786 nm. The source light is fiber guided into a large fish tank of 50L 0.75% Intralipid ($\mu_a = 0.02$ cm $^{-1}$, $\mu_s' = 8.0$ cm $^{-1}$), enabling us to use infinite medium boundary conditions. A detection fiber couples the detected diffusive wave to a fast

avalanche photodiode. A single-sideband demodulator is used to find the homodyne of the signal and the reference wave at 100 MHz. The dynamic range of our current setup is ~ 2500 . The source and detection fiber optics are moved by automated stepper motors. The system is very stable for ~ 3 h.

The experimental geometry is shown in Fig. 1(a). The source position was fixed and taken to be the origin of our coordinate system. As shown in Fig. 1(a), we "made" the detection plane by scanning a single detection fiber over a square region from $(-4.65, -4.65, 5.0)$ cm to $(4.65, 4.65, 5.0)$ cm in a plane at $z_d = 5.0$ cm in steps of size $\Delta x = \Delta y = 0.3$ cm. The amplitude and phase of the DPDW were recorded at each position for a total of 1024 points. We directly measured the amplitude and phase in the homogeneous medium to obtain $U_0(\mathbf{r}_d, \mathbf{r}_s, \omega)$.

Two absorbing slices, each 1.5 cm \times 1.5 cm \times 0.4 cm were then submerged in the turbid medium (0.75% Intralipid). The slices were made of resin plus TiO $_2$ and absorbing dye. Slice 1 with $\mu_{a1} = 0.20$ cm $^{-1}$ was placed at position $(-1.6, -0.3, 3.0)$ cm, and slice 2 with $\mu_{a2} = 0.10$ cm $^{-1}$ was placed at $(1.6, 0.3, 3.0)$ cm. The scattering coefficients of these two slices are the same as that of the background, i.e., 8.0 cm $^{-1}$. We obtained the scattered wave $U_1(\mathbf{r}_d, \mathbf{r}_s, \omega)$ by subtracting the homogeneous background DPDW $U_0(\mathbf{r}_d, \mathbf{r}_s, \omega)$ from the measured signal $U_t(\mathbf{r}_d, \mathbf{r}_s, \omega)$. The 2D Fourier transform $U_1(\mathbf{r}_d, \mathbf{r}_s, \omega)$ leads to the inhomogeneity function $T(p, q, z_j, \mathbf{r}_s, \omega)$ in Eq. (4). We use *a priori* information about the object position(s) in the z direction to select a single image slice, e.g., a slice at $z = z_{obj}$, where the inhomogeneity function is $T(p, q, z_{obj}, \mathbf{r}_s, \omega)$. The 2D inverse Fourier transform of $T(p, q, z_{obj}, \mathbf{r}_s, \omega)$ gives an accurate spatial map of the absorption variations $\delta\mu_a(x, y, z_{obj})$.

The reconstructed images from the experimental data are shown in Fig. 2. The two objects are well resolved (with a peak-trough >2). The reconstructed x - y positions of these two slices are approximately $(-1.80, -0.25)$ cm and $(1.85, 0.25)$ cm, close to their true x - y positions of $(-1.6, -0.3)$ cm and $(1.6, 0.3)$ cm. Inaccuracies in the position measurements might account for the discrepancy. Images shown in Figs. 2(b) and 2(d) are unprocessed. The reconstructed absorption coefficients are well above the background-noise level and close up to the true values [e.g., $\mu_{a1}^{rec} \approx (0.22 \pm 0.03)$ cm $^{-1}$ and $\mu_{a2}^{rec} \approx (0.13 \pm 0.03)$ cm $^{-1}$]. The noise in the reconstruction is mainly from the finite step size and scan region, the positional error, and the electronics. The refractive-index mismatch between the object and the background medium also contributes to the inaccuracy in the reconstructed optical properties. The fast Fourier transform (FFT) calculation takes less than 200 ms of CPU time on a SunSparc10 workstation, and the presence of multiple objects does not increase the computation complexity.

The feasibility of the FFT algorithm for imaging a scattering object was also demonstrated. The geometry is the same as in Fig. 1(a). In this case we used spherical objects as heterogeneities instead of thin slices to test the accuracy of our algorithm for imaging extended objects. Sphere 1, of radius

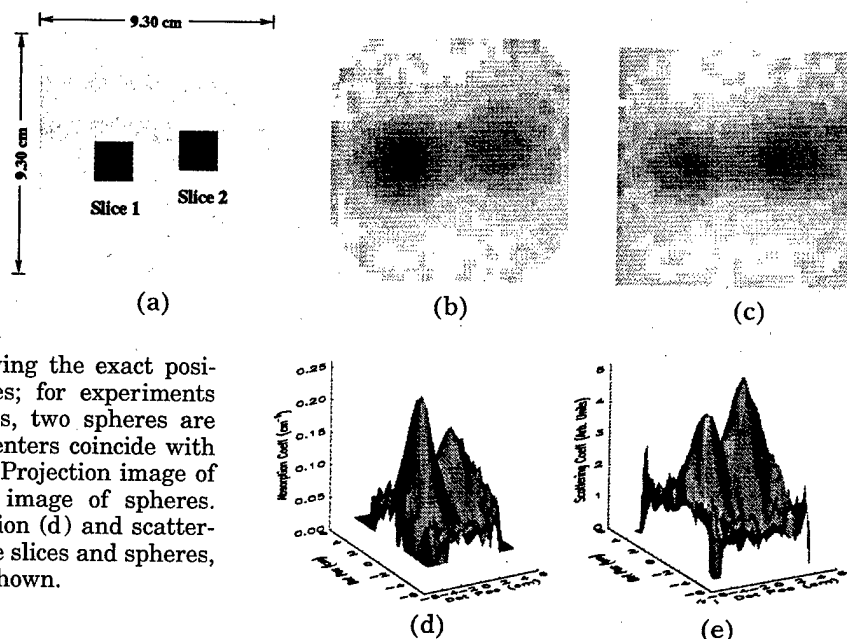


Fig. 2. (a) Slice showing the exact positions of the two slices; for experiments with scattering objects, two spheres are placed so that their centers coincide with the slice centers. (b) Projection image of slices. (c) Projection image of spheres. The recovered absorption (d) and scattering (e) properties of the slices and spheres, respectively, are also shown.

0.75 cm with $\mu_{s1}' \approx 16 \text{ cm}^{-1}$, was placed at $(-1.6, -0.3, 3.0) \text{ cm}$, sphere 2, of the same radius with $\mu_{s2}' \approx 26 \text{ cm}^{-1}$, was placed at $(1.6, 0.3, 3.0) \text{ cm}$. Both spheres have the same absorption coefficient as the background, i.e., 0.02 cm^{-1} . We see from Fig. 2(c) and 2(e) that positional information about these two scattering objects is recovered. In this case we use a slice through the sphere center at $z = z_{\text{obj}}$ and obtain a 2D scattering contrast image. We do not expect to reconstruct the scattering coefficients accurately since the objects are extended. However, we were still able to obtain the correct positions, and the two objects are well resolved [Figs. 2(c) and 2(e)]. Furthermore, the ratio of the reconstructed scattering coefficients is close to the true ratio, i.e., $\mu_{s2}^{\text{rec}}/\mu_{s1}^{\text{rec}} \approx 1.35$, while the true ratio is ~ 1.62 .

Depth information is required for full 3D images with this diffraction tomography technique. One simple method is to use a secondary localization scheme to deduce object depth. Alternatively, two projection images of the sample along orthogonal directions provide sufficient information for 3D reconstruction.

We have successfully applied near-field diffraction tomography, diffuse-photon density waves, and FFT's to obtain projection images of hidden objects in highly scattering tissue phantoms. It may be possible to obtain clinical projection images in real time with this FFT approach. The geometry used so far has been infinite. In practice, boundary effects present important problems. On the one hand, matching materials might be used to reduce the boundary effects. On the other hand, the introduction of a surface integral term in Eq. (1) or better Green's functions (which vanish on the extrapolated boundary) may be used to incorporate boundary effects. The technique presented here provides a basis for more complicated and realistic reconstruction methods to address these issues.

We acknowledge useful discussions with Maureen O'Leary. A. G. Yodh acknowledges support from National Science Foundation grant DMR93-06814. B. Chance acknowledges support in part from the

National Institute of Health grants CA 50766 and CA 60182.

References

1. A. Yodh and B. Chance, *Phys. Today* **48**(3), 34 (1995), and references therein.
2. See related studies in *Advances in Optical Imaging and Photon Migration*, R. Alfano, ed., Vol. 2 of Trends in Optics and Photonics Series (Optical Society of America, Washington, D.C., 1996).
3. M. Tamura, O. Hazeki, S. Nioka, and B. Chance, *Ann. Rev. Physiol.* **51**, 813 (1989).
4. S. R. Arridge, P. van der Zee, M. Cope, and D. T. Delpy, *Proc. SPIE* **1431**, 204 (1991); R. L. Barbour, H. L. Graber, Y. Wang, J. H. Chang, and R. Aronson, in *Medical Optical Tomography: Function Imaging and Monitoring*, G. Müller, ed. (SPIE Optical Engineering Press, 1993), Vol. **IS11**, p. 87; M. A. O'Leary, D. A. Boass, B. Chance, and A. G. Yodh, *Opt. Lett.* **20**, 426 (1995); C. P. Gonatas, M. Ishii, J. S. Leigh, and J. Schotland, *Phys. Rev. E* **52**, 4361 (1995); B. M. Pogue, M. S. Patterson, H. Jiang, and K. D. Paulsen, *Phys. Med. Biol.* **40**, 1709 (1995); H. B. Jiang, K. D. Paulsen, U. L. Osterberg, B. W. Pogue, and M. S. Patterson, *Opt. Lett.* **20**, 2128 (1995).
5. S. Fantini, M. A. Franceschini, G. Gaida, E. Gratton, H. Jess, W. W. Mantulin, K. T. Moesta, P. M. Schlag, and M. Kaschke, *Mod. Phys.* **23**, 149 (1996).
6. A. C. Kak and M. Slaney, *Principles of Computerized Tomographic Imaging* (IEEE Press, New York, 1988), Chap. 7.
7. E. Wolf, *Opt. Commun.* **1**, 153 (1969); E. Wolf, in *Trends in Optics*, A. Consortini, ed. (Academic, San Diego, Calif., 1996), p. 83; J. Devaney, *Inverse Problems* **2**, 161 (1986).
8. D. N. Pattanayak, GE Tech. Info. Series 91CRD241 General Electric; C. L. Matson, N. Clark, L. McMackin, and J. S. Fender, in *Advances in Optical Imaging and Photon Migration*, R. Alfano, ed., Vol. 2 of Trends in Optics and Photonics (Optical Society of America, Washington, D.C., 1996), p. 261.
9. M. S. Patterson, B. Chance, and B. C. Wilson, *Appl. Opt.* **28**, 2331 (1989).
10. A. Baños, *Dipole Radiation in the Presence of a Conducting Half-Space* (Pergamon, New York, 1996), p. 18.